

ac susceptibility and ^{51}V NMR study of MnV_2O_4

S.-H. Baek^{1,2}, K.-Y. Choi¹, A.P. Reyes¹, P.L. Kuhns¹, N.J. Curro², V. Ramachandran¹, N.S. Dalal¹, H.D. Zhou¹, and C.R. Wiebe¹

¹National High Magnetic Field Laboratory, Tallahassee, Florida, 32310

²Los Alamos National Laboratory, Los Alamos, NM, 87545

Abstract. We report ^{51}V zero-field NMR of manganese vanadate spinel of MnV_2O_4 , together with both ac and dc magnetization measurements. The field and temperature dependence of ac susceptibilities show a reentrant-spin-glass-like behavior below the ferrimagnetic(FEM) ordering temperature. The zero-field NMR spectrum consists of multiple lines ranging from 240 MHz to 320 MHz. Its temperature dependence reveals that the ground state is given by the simultaneous formation of a long-range FEM order and a short-range order component. We attribute the spin-glass-like anomalies to freezing and fluctuations of the short-range ordered state caused by the competition between spin and orbital ordering of the V site.

PACS numbers:

Submitted to: *J. Phys.: Condens. Matter*

1. Introduction

For several decades, transition-metal spinels of AB_2X_4 type have been a subject of active research because of the intriguing nature of the underlying physics [1]. The many unusual phenomena found in the spinel compounds are due primarily to the corner-shared tetrahedral network of the B cations which resembles the geometrically frustrated pyrochlore lattice. The magnetic properties of spinels rely heavily on whether the B cations have orbital degrees of freedom, and whether the A cations are magnetic or nonmagnetic.

Among the vast number of spinels, manganese vanadate MnV_2O_4 [2, 3] is one of the fascinating but very complex compounds to understand. This is because (i) the V^{3+} ion ($3d^2$, $S = 1$) possesses orbital degeneracy in its t_{2g} orbital; the orbital ordering being a common feature found in other insulating vanadates ($A = \text{Zn}$ [4], Mg [5], Cd [6]); and (ii) both the A and B sites are magnetic as in manganese chromite, MnCr_2O_4 [7, 8].

One may expect that MnV_2O_4 shares common features with MnCr_2O_4 as well as with other vanadium spinels. Indeed, MnV_2O_4 undergoes long-range FEM ordering at 56 K and the spin configuration of the B sites changes from collinear to non-collinear

triangular type at low temperature (T), as found in MnCr_2O_4 [8]. Like other vanadate spinels, MnV_2O_4 also undergoes two successive phase transitions – orbital order and magnetic long-range order. Interestingly, in the case of MnV_2O_4 , the cubic-to-tetragonal structural transition related to the orbital order takes place at $T_S = 53$ K, just below the FEM transition temperature $T_C = 56$ K [3]. Here the question arises about the combined effect of the two features (i) and (ii) on a ground state. However, this issue has not yet been thoroughly addressed.

In this paper, we report the observation of the complex ground state in MnV_2O_4 through ac/dc magnetization and zero-field (ZF) ^{51}V NMR measurements. Our data reveal that there exists a short-range ordered state on top of the long range FEM order, leading to a spin-glass-like behavior. They are discussed in terms of the competing spin and orbital ordering of the V^{3+} ion.

2. Sample preparation and experimental details

Polycrystalline powder sample of MnV_2O_4 was prepared by standard solid-state reaction. Stoichiometric mixtures of MnO and V_2O_3 were ground together and pressed into pellet, the pellet was placed into an evacuated quartz tube ($\sim 10^{-5}$ torr) and fired for 40 hours at 950 °C. Samples were characterized by X-ray powder diffraction. Both dc and ac susceptibility measurements were performed as a function of both field and temperature using SQUID magnetometer (Quantum Design MPMS). An applied frequency was in the range of $10^{-1} - 10^3$ Hz with a driving field magnitude of 5 Oe. NMR experiments were carried out at zero external field using a coherent pulsed spectrometer capable of computer-controlled tuning of a probe which is calibrated over a wide frequency range. In preliminary measurements using an untuned NMR probe ($Q = 1$), we detected two groups of signals at near 280 MHz and 560 MHz at 4.2 K. These were assigned to the NMR signals of V^{3+} and Mn^{2+} ions, respectively. A probe with tank circuit was subsequently employed to focus on the stronger signal of the V site. The ^{51}V NMR spectra were obtained by integrating averaged spin echo signals as the frequency was swept through the resonance line.

3. Results and discussion

3.1. Magnetic susceptibilities

Figure 1 shows the temperature dependence of the dc susceptibility under an applied field of 300 Oe together with the ac susceptibility at a frequency of 1 Hz. The field-cooled (FC) and zero-field-cooled (ZFC) curves display a pronounced bifurcation below the FEM ordering temperature of T_C . As T_C is approached from above, the FC curve increases steeply and then shows a dip around the structural phase transition temperature at T_S and finally increases monotonically. In contrast, the ZFC curve exhibits a maximum and then a monotonic decrease upon cooling from T_C . Our results are in a good agreement with Ref. [3]. Noticeably, one observes a substantial difference

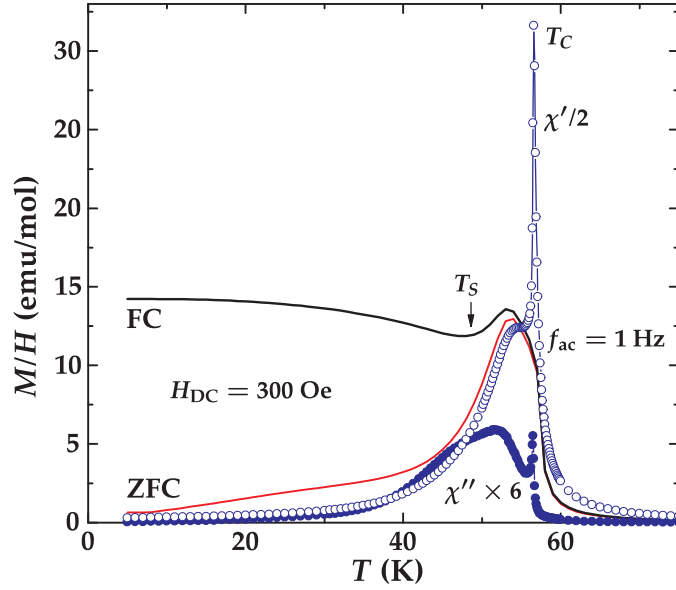


Figure 1. (Online color) Temperature dependence of the ac (circle symbols) and dc (solid lines) susceptibilities of MnV_2O_4 . For clarity, the real and imaginary part of the ac susceptibilities are divided by 2 and multiplied by 6, respectively.

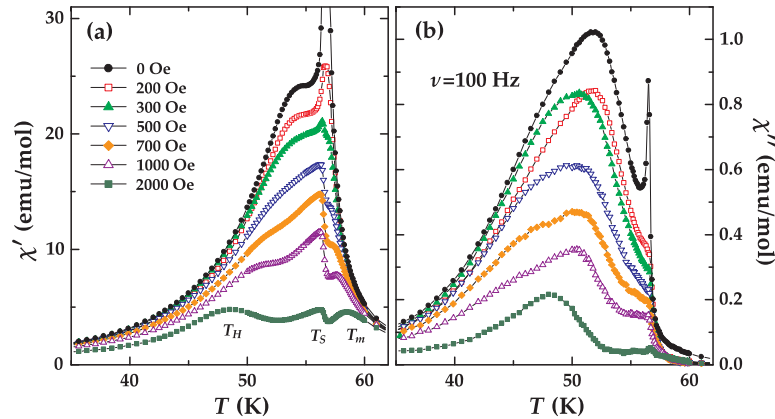


Figure 2. (Color online) Field dependence of the real (a) and imaginary (b) parts of the ac susceptibility of MnV_2O_4 as a function of temperature. A field is driven at $H_{ac} = 5$ Oe and $\nu = 100$ Hz.

between the ac and ZFC dc susceptibilities below T_C , implying the presence of reentrant-spin-glass (RSG)-like anomalies.

In figure 2 we present the temperature dependence of the ac susceptibilities, $\chi(H_a, T)$ for different static field H_a applied parallel to the ac driving field. With decreasing temperature the real part of $\chi(H_a, T)$ exhibits a sharp peak around T_C and then a round maximum and finally falls off upon further cooling. With increasing H_a , the latter maximum (designated by T_H) decreases in both amplitude and temperature. This so-called Hopkinson maximum is not critical in origin, but arises from processes associated with the regular/technical contributions to the susceptibility (for example, domain wall motion and coherent rotation) [9]. The former sharp peak develops to two

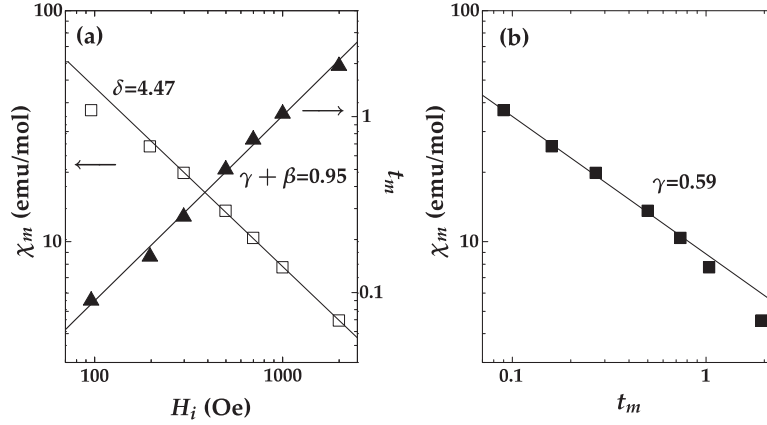


Figure 3. (a) The critical field amplitude versus the internal field (open square) is presented together with the reduced temperature versus the internal field (full triangle) on a double-logarithmic scale. (b) A double-logarithmic plot of the critical field temperature versus the reduced temperature. The solid and dotted lines are a fit to Eqs. (1)-(3).

peaks (denoted by T_m and T_S , respectively) with increasing dc field. The peak T_m is suppressed in amplitude and shifts to higher temperature with an increase in the dc field. This is due to critical fluctuations accompanying a transition from a paramagnetic to a FEM state [10]. In contrast, the peak T_S decreases in amplitude without showing any shift in temperature. This might be associated with the structural phase transition [3], leading to a pinning of domain walls. The imaginary part of $\chi(H_a, T)$ shows a sharp peak around T_C , which exhibits a similar behavior as the peak T_S . In addition, the loss peak of $\chi''(H_a, T)$ shows up around 51 K, which is suppressed in both temperature and amplitude as T_a increases.

Since the peak T_m is governed by critical fluctuations, it is expected to follow the static scaling law. The field and temperature dependence of the critical peak is related to the standard critical exponents [11, 12, 13] by

$$\chi(H_i, T_m) \propto H_i^{1/\delta-1} \quad (1)$$

$$t_m \propto H_i^{(\gamma+\beta)^{-1}} \quad (2)$$

$$\chi(H_i, T_m) \propto t_m^{-\gamma}, \quad (3)$$

where H_i is the internal field given by $H_a = H_i - NM$ where N is the demagnetizing factor and M is the magnetization. In our case, N is estimated by the slope of the low field shearing curves around T_C (not shown here). t_m is the reduced temperature defined as $t_m = (T_m - T_C)/T_C$. We determine the temperature of $T_C = 56.58$ K from the zero field data. The critical field amplitude $\chi(H_i, T_m)$ is directly obtained from Fig. 2(a). In Fig. 3 we provide a double-logarithmic plot of $\chi(H_i, T_m)$ versus H_i , t_m versus H_i , and $\chi(H_i, T_m)$ versus t_m , respectively. A close look at the data reveals a small curvature at low fields. This is typical for the system with exchange coupling strength disorder [10]. A least squares fit of the data between the restricted fields yield the exponent values of

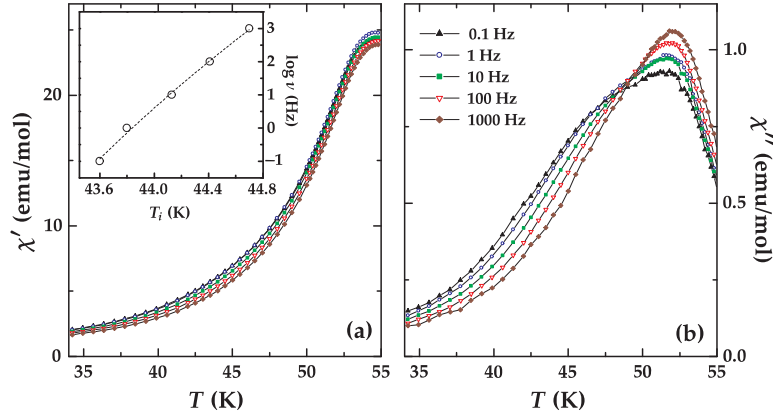


Figure 4. (Color online) Frequency dependence of the real (a) and imaginary (b) parts of the ac susceptibility as a function of temperature. Inset: Frequency shift of the inflection point of the real part of the susceptibility versus temperature.

$\delta = 4.47 \pm 0.05$, $\gamma + \beta = 0.95 \pm 0.04$ and $\gamma = 0.59 \pm 0.03$. The δ and β values are close to the prediction of a 3D Heisenberg model [12]. However, the γ value strongly deviates from it. Although we cannot exclude the uncertainties in evaluating exponents, it might be ascribed to a first-order-like transition due to strong spin-orbital coupling as well as to a competition between frustration and a structural phase transition (see below).

In figure 4 the temperature dependence of the $\chi'(T)$ and $\chi''(T)$ is presented as a function of frequency in the range of $10^{-1} - 10^3$ Hz. Both $\chi'(T)$ and $\chi''(T)$ exhibit pronounced frequency dependence between 20 K and T_C . Overall, with increasing frequency both $\chi'(T)$ and $\chi''(T)$ shifts to higher temperature. This is unexpected for a long-range ordered FEM state, implying that a spin freezing phenomenon takes place in the FEM ordered background.

The shift of the ac susceptibility as a function of the frequency is estimated by taking the inflection point of $\chi'(T)$ [see the inset of figure 4(a)]. From the maximal shift ΔT_i we obtain the value of $\varphi = \Delta T/T_i \Delta(\log \omega) \sim 0.007$. For a spin glass the value is typically of the order of 10^{-2} , while for a superparamagnet it lies between $10^{-1} - 10^{-2}$ [14]. Using this criterion, we conclude that the studied compound belongs to a class of a spin glass. Further, we fit the experimental data in terms of the Vogel-Fulcher law $\omega = \omega_0 \exp[-E_a/k_B(T_i - T_0)]$ to figure out the nature of the spin freezing process. It yields the values of $\omega_0 \approx 10^{33}$ Hz, $E_a \approx 287$ K, and $T_0 \approx 33.5$ K. The unrealistic large value of ω_0 suggests that the spin freezing is not of simply cooperative but governed by an intricate process.

3.2. NMR measurements

^{51}V zero-field NMR spectrum and its temperature evolution are shown in figure 5(a) for slow cooling (SC), with the rate of ~ 1 K/min, and in figure 5(b) for rapid cooling (RC), with the rate of 60 K/min. The Boltzmann correction for the signal intensities has been made by multiplying each spectrum by T . The spectrum has a complex structure and

spans a wide range of frequencies from 240 to 320 MHz. The resonance frequency in zero field is given as $\gamma_N H_{\text{hf}}$ where γ_N ($= 11.193 \text{ MHz/T}$) is the nuclear gyromagnetic ratio. The hyperfine field H_{hf} is dominated by the core polarization of the inner s -electrons by the outer unpaired d -electrons. For the V^{3+} ion ($3d^2$, $S = 1$), the estimated H_{hf} due to pure Fermi contact is about $\sim 25 \text{ T}$ [15] which falls into $\sim 280 \text{ MHz}$ range. The contributions from transferred, dipolar, or orbital hyperfine fields are negligible.

One can infer from figure 5 that the ^{51}V NMR line is composed of several overlapping structures, whose peaks are somewhat resolved. This is not surprising given the low crystal symmetry [16]. One possibility is the quadrupole interactions split the ^{51}V ($I = 7/2$) degenerate levels producing $2I = 7$ transitions. However we discard this model since the quadrupole coupling required to represent the spectrum would be too large for the V nucleus. Hence, we attribute the structures to V sites belonging to several magnetically differentiated sites.

The temperature dependence of the integrated intensity multiplied by T of the spectrum is shown in figure 5 (c) for both SC and RC. The signal for the RC case can be observed even above T_C while the signal for SC becomes very weak near 40 K. The loss of NMR signal intensity at high T is due to the fast spin fluctuations i.e., shortening of T_2 associated with magnetic ordering. The different temperature dependence of the signal intensity for different cooling rate points to the effects of disorder which influences the freezing rate of the short-range correlated spins, a conclusion also deduced previously from the magnetization results. At low $T < 20 \text{ K}$, however, the signal intensity and shape are the same regardless of the cooling rate implying that the spin ground state of this compound is not affected by the thermal history. This is consistent with the ac susceptibility results, which show no frequency dependence at the same temperature range.

By examining the evolution of the spectrum in figure 5 (a) and (b), we take note that the NMR peak near 265 MHz is quite distinguishable from the other lines, and survives after the disappearance of the other lines at high temperature. Also we see that the shift of the NMR line is very small, if any, up to temperature near T_C . This is surprising since the NMR resonance frequency usually follows the bulk magnetization which often shows gradual second order transition behavior. Therefore, the NMR data suggest that the magnetic transition at T_C must be of first order.

In both SC and RC cases, the stable configuration is established below 15 K as shown in figure 5. Here we show that the intriguing ground state is expected in the presence of several competing interactions. Spinels contain two different exchange coupling constants: J_{AB} and J_{BB} between the A and B and the B and B sites, respectively. For a cubic phase, a magnetic configuration relies on the parameter u defined as [17]

$$u = \frac{4J_{\text{BB}}S_{\text{B}}}{3J_{\text{AB}}S_{\text{A}}}, \quad (4)$$

where S_{A} and S_{B} are spin magnitudes at the respective A and B sites. The relative strength of two interactions determines a ground state. For example, the ground state

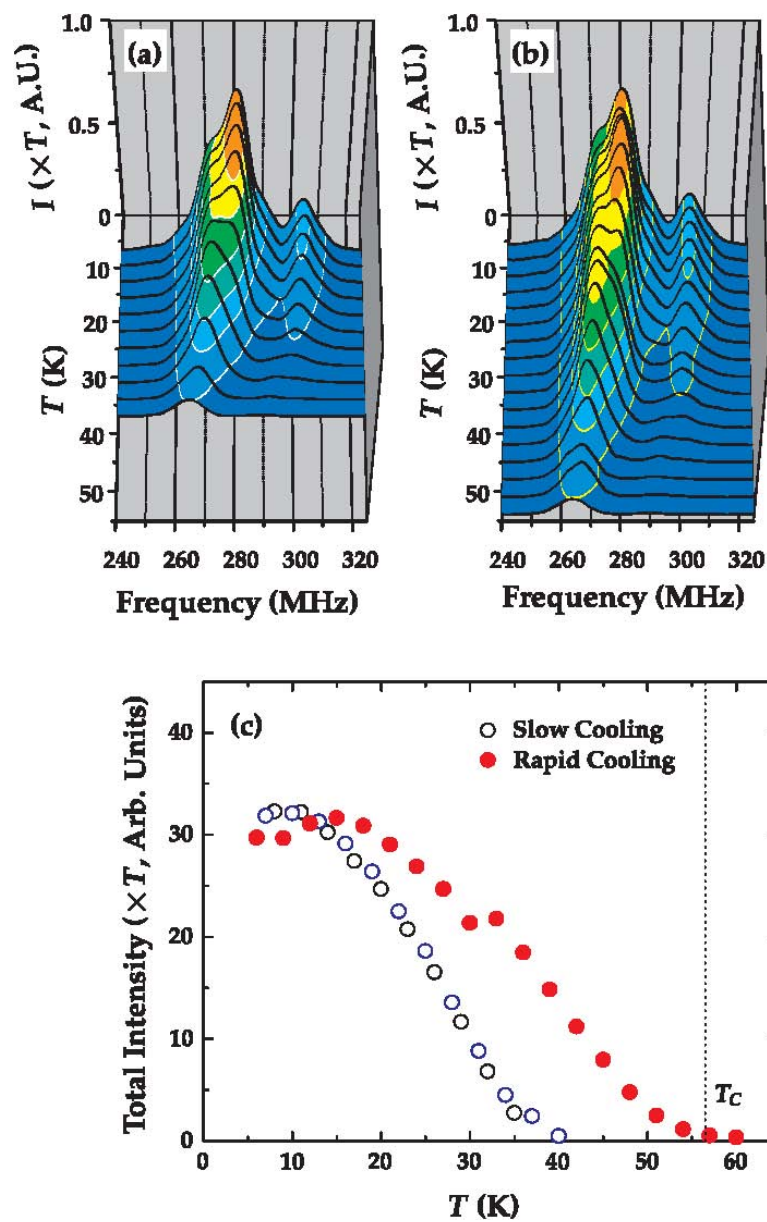


Figure 5. (Online color) (a) Evolution of the NMR spectrum with increasing T in ZF for slow cooling condition. The Boltzmann correction for intensity was taken into account by scaling each spectrum by T . (b) For rapid cooling, the evolution of the spectral shape is the same except the observation of the signal at much higher temperature. (c) Total integrated intensity of the NMR signal in zero field was plotted against temperature for slow and rapid cooling. Note that, for rapid cooling, the signal was detected even above T_C .

of chromites $[\text{Co},\text{Mn}]\text{Cr}_2\text{O}_4$ with $u = 1.5 - 2.0$ shows a coexistence of FEM long-range order and spiral short-range order that causes the RSG-like behavior [8]. The MnV_2O_4 system seems to lie in the same parameter range as suggested by the fact that the RSG-like behavior starts to appear at T_C of the cubic phase (see figure 1).

In $[\text{Co},\text{Mn}]\text{Cr}_2\text{O}_4$ the appearance of the short-range order is ascribed to the residual magnetic frustration in the B site, which is non-vanishing when J_{AB} is smaller than J_{BB} . In our case, however, this scenario seems to be less plausible since the frustration could be relieved through the orbital ordering of the V^{3+} ions. Rather, the short-range character in MnV_2O_4 may be due to the specific orbital ordering that occurs at T_S . In the cubic phase ($T > T_S$) the t_{2g} orbitals are degenerate and thus the orbital degrees of freedom are irrelevant. The V sublattice aligns ferromagnetically due to the antiferromagnetic couplings between V^{3+} and Mn^{2+} ions. In contrast, in the tetragonal phase ($T < T_S$), a structural phase transition takes place to one whose orbital configuration is intimately coupled to a spin configuration via a orbital-spin coupling [3]. Accordingly, an antiferro-orbital arrangement of the V^{3+} ions is preferred due to the dominant ferromagnetic interaction between V^{3+} ions.

This staggered-type orbital configuration of MnV_2O_4 is contrasted to the orbital patterns found in vanadium spinels ($\text{A}=\text{Zn},\text{Mg},\text{Cd}$), which are the nonmagnetic analogue of MnV_2O_4 in the A site [18, 19, 20]. Tsunetsugu and Motome [18] suggested alternating $d_{xy}-d_{xz}$ and $d_{xy}-d_{yz}$ orbital chain structure, which is compatible with the space group $I4_1/a$. On the other hand, Tchernyshyov [19] argued against the above model and proposed the space group $I4_1/amd$ which is associated with a complex linear combination of d_{xz} and d_{yz} orbitals. Regardless of the detailed picture, the one-dimensional antiferromagnetic chain is the essential ingredient to both models owing to the direct overlap of d_{xy} orbitals [4]. This means that the orbital ordering imposed by the exchange couplings of $\text{V}^{3+}-\text{Mn}^{2+}$ ions is different from the orbital pattern favored by the structural phase transition. This causes the instability of the antiferro-orbital configuration. Although frustration is relieved through the structural phase transition, it also paves the way for the competing orbital ordering of V^{3+} ions to occur.

Lastly, we present the external field (H) dependence of the NMR spectrum in figure 6. We observe that each identified line at zero field does not shift at all with H . Instead, amplitude of each peak decreases or increases without shift in such a way that the first moment (M_1) or the center of gravity of the spectrum changes linearly with increasing H as shown in figure 6 (c). Moreover, new NMR lines appear as H increases. The slope of M_1 versus H is initially 5.4 MHz/T but get bigger smoothly up to 3 T being fixed to 7 MHz/T. The value is still smaller than the gyromagnetic ratio γ_N of V (11.193 MHz/T). We conjecture that this behavior may be possible only with assumption of the discrete spin directions which is distributed spatially. The change of the slope below 3 T may be due to the effect of the rotation of the domain or the similar stabilized process against the external field.

Also we observed that the total intensity of the spectrum increases with increasing H up to 4 T above which it is saturated [see figure 6 (b)]. Typically, NMR signal

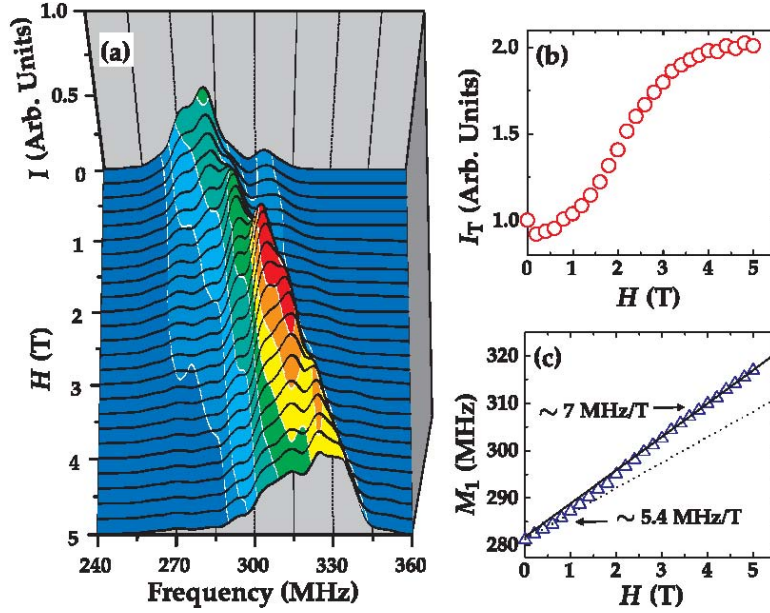


Figure 6. (Online color) (a) External field dependence of spectrum up to 5 T. (b) Total integrated intensity increases with external field saturating at ~ 4 T. (c) First moment versus external field. The initial slope of 5.4 MHz/T changes to 7 MHz/T at higher fields. The value must be compared to the expected value of 11.193 MHz/T.

enhancement is associated with the domain walls which are swept out with H resulting in the disappearance of the enhancement effect. In this regard, the usual enhancement of the signal with large H suggests the persistence of the domain motions at least up to 4 T. Since the domains of the long-range ordered phase are expected to be frozen-in at low fields, the enhanced high-field signal might be related to the domain motions of the short-range ordered state. Above we have ascribed the short-range order to the orbital ordering induced by the structural phase transition. Specifically, the V ions form the antiferromagnetic chain with the exchange coupling constant of an order of 1000 K [3]. In this situation, the short-range ordered component of the V spins is frustrated. Thus, in the studied field range the short-range ordered state undergoes a minor change in the spin directions accompanying the domain motions. To draw the more concrete picture on the puzzling behavior of the field dependence, a further study of the single crystal is needed.

Within our study, we cannot determine the exact nature of the short-range ordered ground state. More direct determination has to come from a neutron diffraction study. However, it cannot be identified as a classical spin glass phase because its NMR signal intensity is comparable to that of the long-range ordered phase. It is possible that the RSG-like behavior is associated with the FEM domains and is a consequence of the freezing of fluctuations of the short-range ordered state.

4. Conclusion

In conclusion, we examined the ground state of MnV_2O_4 through magnetization and NMR measurements. We observed the reentrant-spin-glass-like behavior on top of the long-range FEM order. Our study provides a clear-cut example of the inhomogeneous ground state in *undoped* compounds where spin interactions and orbital ordering related to a structural phase transition are two competing parameters.

Acknowledgments

This work was supported by NSF in-house research program State of Florida under cooperative agreement DMR-0084173.

References

- [1] P.G. Radaelli. *New J. Phys.*, 7:53, 2005.
- [2] R. Plumier and M. Sougi. *Physica B*, 155:315, 1989.
- [3] K. Adachi, T. Suzuki, K. Kato, K. Osaka, M. Takata, and T. Katsufuji. *Phys. Rev. Lett.*, 95:197202, 2005.
- [4] S.-H. Lee, D. Louca, H. Ueda, S. Park, T.J. Sato, M. Isobe, Y. Ueda, S. Rosenkranz, P. Zschack, J. Iniguez, Y. Qiu, and R. Osborn. *Phys. Rev. Lett.*, 93:156407, 2004.
- [5] H. Mamiya, M. Onoda, T. Frubayashi, J. Tang, and I. Nakatani. *J. Appl. Phys.*, 81:5289, 1997.
- [6] M. Onoda and J. Hasegawa. *J. Phys.: Cond. Matt.*, 15:L95, 2003.
- [7] J.M. Hastings and L.M. Corliss. *Phys. Rev.*, 126:556, 1962.
- [8] K. Tomiyasu, J. Fukunaga, and H. Suzuki. *Phys. Rev. B*, 70:214434, 2004.
- [9] S. Chikazumi. *Physics of Ferromagnetism*. Oxford, Clarendon, 1997.
- [10] G. Williams. In R.A. Hein, editor, *Magnetic Susceptibility of Superconductors and Other Spin Systems*, New York, 1991. Plenum.
- [11] H.E. Stanley. *Introduction to Phase Transitions and Critical Phenomena*. Oxford, Clarendon, 1971.
- [12] M. Campostrini, M. Hasenbusch, A. Pelissetto, P. Rossi, and E. Vicari. *Phys. Rev. B*, 65:144520, 2002.
- [13] H. H. Zhao, H. P. Kunkel, X. Z. Zhou, G. Williams, and M. A. Subramaniam. *Phys. Rev. Lett.*, 83:219, 1999.
- [14] J. A. Mydosh. *Spin glasses: An Experimental Introduction*. Taylor and Francis, London, 1993.
- [15] A.J. Freeman and R.E. Watson. In G.T. Rado and H. Suhl, editors, *Magnetism IIA*, New York, 1965. Academic.
- [16] Fe^{57} NMR in Fe_3O_4 (magnetite) gave rise to 24 lines corresponding to the total number of Fe sites in the monoclinic unit cell at low temperature [21].
- [17] N. Menyuk, K. Dwight, D. Lyons, and T.A. Kaplan. *Phys. Rev.*, 127:1983, 1962.
- [18] H. Tsunetsugu and Y. Motome. *Phys. Rev. B*, 68:060405(R), 2003.
- [19] O. Tchernyshyov. *Phys. Rev. Lett.*, 93:157206, 2004.
- [20] S. Di Matteo, G. Jackeli, and N.B. Perkins. *Phys. Rev. B*, 72:020408(R), 2005.
- [21] P. Novák, H. Štěpánková, J. Englich, J. Kohout, and V.A.M. Brabers. *Phys. Rev. B*, 61:1256, 2000.